pH Dependence of Light-Driven Proton Pumping by an Archaerhodopsin from Tibet: Comparison with Bacteriorhodopsin

Ming Ming,* Miao Lu,† Sergei P. Balashov,‡ Thomas G. Ebrey,† Qingguo Li,§ and Jiandong Ding*
*Key Laboratory of Molecular Engineering of Polymers, Department of Macromolecular Science, Fudan University, Shanghai, China; †Department of Biology, University of Washington, Seattle, Washington; ‡Department of Physiology and Biophysics, University of California, Irvine, California; and §Department of Physiology and Biophysics, School of Life Sciences, Fudan University, Shanghai, China

ABSTRACT The pH-dependence of photocycle of archaerhodopsin 4 (AR4) was examined, and the underlying proton pumping mechanism investigated. AR4 is a retinal-containing membrane protein isolated from a strain of halobacteria from a Tibetan salt lake. It acts as a light-driven proton pump like bacteriorhodopsin (BR). However, AR4 exhibits an ''abnormal'' feature—the time sequence of proton release and uptake is reversed at neutral pH. We show here that the temporal sequence of AR4 reversed to ''normal''—proton release preceding proton uptake—when the pH is increased above 8.6. We estimated the pK_a of the proton release complex (PRC) in the M-intermediate to be ~8.4, much higher than 5.7 of wide-type BR. The pH-dependence of the rate constant of M-formation shows that the pK_a of PRC in the initial state of AR4 is ~10.4, whereas it is 9.7 in BR. Thus in AR4, the chromophore photoisomerization and subsequent proton transport from the Schiff base to Asp-85 is coupled to a decrease in the pK_a of PRC from 10.4 to 8.4, which is 2 pK units less than in BR (4 units). This weakened coupling accounts for the lack of early proton release at neutral pH and the reversed time sequence of proton release and uptake in AR4. Nevertheless the PRC in AR4 effectively facilitates deprotonation of primary proton acceptor and recovery of initial state at neutral pH. We found also that all pK_as of the key amino acid residues in AR4 were elevated compared to those of BR.

INTRODUCTION

Earlier, a new claret-membrane protein similar to the purple-membrane pigment bacteriorhodopsin (BR) was found in a strain of halobacteria, *H. sp. xz515*, isolated from a salt lake in Tibet (1). In contrast to BR, this pump exhibited a reversed order of light-driven proton release and uptake at neutral pH (1). Its amino acid sequence has been determined (2,3) and this pigment was classified as an archaerhodopsin (AR), a name initially given by Mukohata et al. (4–7) for the BR-like pigments isolated from two Australian strains, *Halobacteria sp. Aus-1* and *Aus-2*, and called AR1 and AR2, respectively. Compared with BR-containing strains such as R1M1 which yield the conventional, ''standard'' BRs, these two strains are from a different genera of *Halobacteriacea*. The AR-containing strains belong to *Halorubrum*, whereas those for BRs are from *Halobacterium* (4,8). A third related pigment found in *Halorubrum sodomense* was named AR3 (8,9); its sequence has been determined by Ihara et al. (8). The pigment from the strain *H. sp. xz515* exhibits 87% sequence similarity to AR1, 97% to AR2, and 84% to AR3, whereas just 59% to BR. It is likely that *H. sp. xz515* is also a member of *Halorubrum*. Hence we name the associated pigment as archaerhodopsin 4 (AR4). The underlying mechanism of its proton pump and the origin of its differences with BR are quite interesting and help elucidate the general features of proton pumps of archaea.

AR4 is localized in the ''claret'' membrane as a patch in the plasma membrane. SDS-page electrophoresis shows that AR4 is the only protein in the claret membrane. Although data on AR4 is limited, much information on BR is available, which is helpful for a comparative study (10–14) (see also two special journal issues on BR (15,16)). The chromophore of BR, retinal, is covalently bound to Lys-216 of the apoprotein via a protonated Schiff-base. Upon excitation with a photon, the retinal is isomerized from the all-*trans* to 13-*cis* configuration, which initiates a photocycle that goes through a series of photointermediates with characteristic absorption maxima (17):

$$bR_{570} \xrightarrow{h\nu} K_{610} \leftrightarrow L_{550} \leftrightarrow M_{412} \leftrightarrow N_{560} \leftrightarrow O_{640} \rightarrow bR_{570}.$$

Detailed spectroscopic studies show that most intermediates include two or more substates, some of which are of great importance for the mechanism (12,18–21). The photocycle is coupled to the unidirectional transfer of a proton. During a photocycle, one proton is released to the extracellular side and another proton is taken up from the cytoplasmic side.

Because of its simplicity and importance as a proton pump, BR is one of the best studied membrane proteins, and it is often used as a model of membrane and energy transducing proteins (e.g., 22–29). Studies of the kinetics of proton translocation across the membrane show that at neutral pH, light-induced proton transfer from the Schiff base to Asp-85 during the L-to-M transition leads to prompt proton release (on a submillisecond timescale) from the proton release complex (PRC or XH) to the extracellular surface (30–32). It is thought that the PRC consists of several amino acid residues, primarily Glu-194 and Glu-204, as well as water molecules (33–37). Most recently, Garczarek et al. identified a protonated water cluster surrounded by six side

Submitted October 22, 2005, and accepted for publication January 19, 2006.
Address reprint requests to Jiandong Ding, E-mail: jding1@fudan.edu.cn.

0006-3495/06/05/3322/11 $2.00
doi: 10.1529/biophysj.105.076547

chains and three backbone groups (Tyr-57, Arg-82, Tyr-83, Glu-204, Glu-194, Ser-193, Pro-77, Tyr-79, and Thr-205) and suggested that this complex might be responsible for the proton release of wild-type (WT) BR (38). After proton release, proton uptake occurs in the $N_{560} \rightarrow O_{640}$ transition (39) or between two N-substates (40), usually in a time of the order of a few milliseconds. Therefore, proton pumping by BR under physiological conditions results in a unidirectional proton release at the extracellular side followed by proton uptake at the cytoplasmic side.

Several polar or charged residues located in the proton channel are highly conserved in all members of the BR and AR families which are proton pumps (8,9). The associated pK_as of these groups must be altered during proton transfer, and thus pH titrations are very useful for elucidating proton pumping mechanisms of BR and BR-like proteins. In BR, Asp-85 is the primary acceptor of the Schiff-base proton. Its pK_a changes in the photocycle by several pK units (41–43). The pK_a of the PRC is quite high (~9.7) (42) in the unphotolyzed state and decreases to 5.7 upon the protonation of Asp-85 (39,44). At neutral pH, this would lead to its deprotonation. The protonation of Asp-85 is closely coupled to the dissociation of a proton from PRC at neutral pH, and proton release from the PRC is the result of proton transfer from the Schiff base to Asp-85 upon formation of M. The thermodynamic equilibrium of acid-base transitions between the two interacting groups predicts that the changes in the pK_a of Asp-85 are linked to the opposite changes in the pK_a of the PRC (42,45–47). This coupling underlines the fast light-induced proton release in BR at pH levels between 6 and 9 (19,42).

In contrast to BR, we found a different sequence of light-induced proton uptake and release at neutral pH in AR4 (1). AR4 is offered by nature as a version of proton pumping machine with all key amino acids residues implicated in proton transport in BR conserved. A series of interesting questions can be raised: What is the cause of the reversed proton pumping behaviors of this protein? It is known that the order of proton release and uptake in BR can be reversed by decreasing the medium pH sufficiently (44). Then if both AR4 and BR operate on similar basic principles (48), could the time order in AR4 be analogously reversed when the medium pH is raised? Is the PRC of AR4 still functional in the photocycle? The answers would be helpful in understanding the mechanism of proton pumping proteins more deeply.

In this work, we compared the main features of the two pigments. The pH-dependence of the photocycle and proton pumping by AR4 were examined. Although fast light-induced proton release was blocked below pH 8.2, it was observed at higher pHs. The pK_as of the initial proton acceptor from the Schiff base, of the proton release complex in different states, and of the proton donor to the deprotonated Schiff-base were determined. We found that all pK_as of the key amino acid residues in AR4 were elevated compared to those of BR and that the coupling between protonation of Asp-85 and deprotonation of XH in the M-intermediate of AR4 was weakened. The origin of the reversed temporal order of proton release and uptake in AR4 at neutral pH and other differences with BR and other archael proton pumps are also discussed.

MATERIALS AND METHODS

Sample preparation

Bacteria culture and membrane isolation followed the standard procedures for BR (49,50). The BR purple membrane was isolated from R1M1, a *Halobacterium* strain. The culturing of *H. sp. xz515* was reported earlier (1). A suspension of AR4 in the ''claret'' membrane was obtained from the strain *H. sp. xz515* by the same procedure as used for purifying the purple membrane from *H. salinarum* (49,50). A sucrose density step gradient, with concentrations (wt %) of sucrose of 30%, 35%, 40%, and 45%, was employed to purify the claret membrane. After centrifuging the sample (35000 r/min, in the SW41 rotor of a Beckman centrifuge for 12 h), the claret membrane was found in the 40% sucrose layer. It was collected and washed for later use. Besides archaerhodopsin, the claret membrane contained the carotenoid bacterioruberin, which did not separate from AR4 under our purification method; this association had previously been seen for other archaerhodopsins (5,51).

Absorption spectra

Absorption spectra and kinetics of dark adaptation were measured with a Cary-Aviv 14 DS spectrophotometer (Aviv Associates, Lakewood, NJ) as previously described (46). Titration of the purple-to-blue transition was done for dark-adapted samples.

Flash-induced proton pumping behavior

The flash-induced proton release and uptake was detected by the absorption change of pH-sensitive dyes, pyranine and thymol blue, at 456 nm. The signal without a dye was subtracted from that with the dye. The thymol blue as well as pyranine can be separated from AR4 pigment by centrifugation at $25{,}000 \times g$ for 30 min, which indicates that the dyes are not absorbed on the membranes.

Flash-induced transient absorbance changes

The pH-dependence of proton release and proton uptake was measured with a kinetic spectrophotometer constructed (52–55) similar to that described by Govindjee et al. (56). The actinic flash was provided from a camera photoflash through an optical filter with light around 570 nm transmitted. The measuring light is a relatively weak but constant beam, perpendicular to the direction of the flash.

Other measurements such as the pH-dependence of M-formation, pH-dependence of the formation, and decay of O-intermediate, were obtained with another home-built kinetic spectrophotometer as described by Balashov et al. (57). Actinic illumination at 532 nm was provided by a frequency-doubled Quanta Ray DCR-11 Nd-YAG laser (Spectra Physics, Mountain View, CA). The transient signals were digitized using a LeCroy transient recorder. The instrument was controlled by a computer program written in Lab View. Gels were prepared as described by Liu et al. (58) and were incubated at a given pH for at least 12 h. Light adaptation was carried out by illumination with a 500 W projector (430–550 nm) for 5 min. The measurements of photocycle kinetics were performed for light-adapted samples.

All measurements were performed at room temperature unless otherwise indicated.

RESULTS

Proton pumping behavior of AR4

Flash-induced transient proton release and uptake in AR4 was detected by the absorption changes of the pH-sensitive dye pyranine at 456 nm as shown in Fig. 1. An increase of absorption at 456 nm corresponds to proton uptake by the membranes, whereas a decrease at 456 nm reflects proton release. Fig. 1 *A* confirms our earlier observation that in contrast to BR, the light-driven proton pump of AR4 first takes up a proton and then releases a proton (1). The pyranine signal was eliminated in the presence of a buffer (10 mM tris-HCl, pH 7.1) indicating that it originates from a transient light-induced change of the proton concentration in the medium.

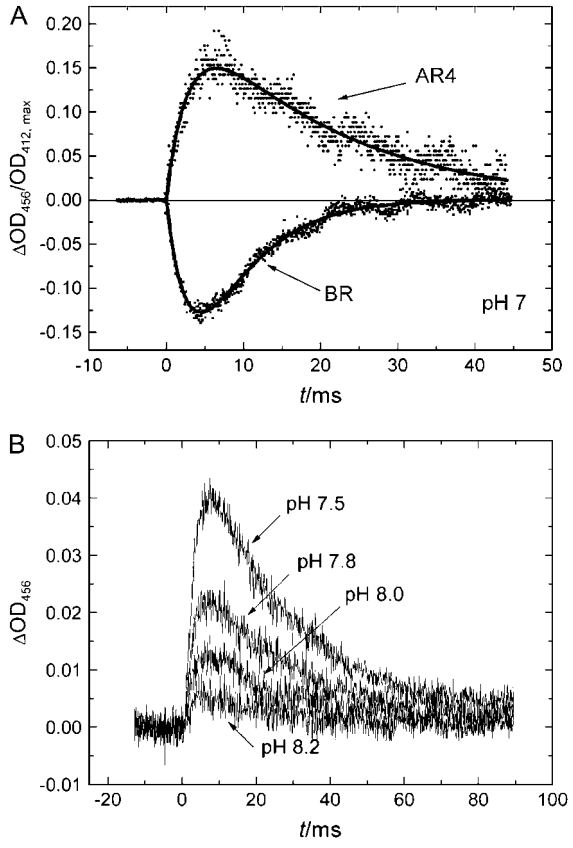

FIGURE 1 (*A*) Flash-induced absorption changes of the pH-sensitive dye pyranine in suspensions of BR or AR4, detected at 456 nm. The absorption changes obtained as a difference between traces taken after and before addition of pyranine. ΔOD_{456} are normalized to $OD_{412,max}$, the amount of flash-induced M-intermediate formed in the photocycle of each protein. The downward curve corresponds to acidification of the medium (proton release first), whereas the upward curve corresponds to proton uptake. Samples were measured in 150 mM KCl aqueous solution containing 25% glycerol. (*B*) pH-dependence of flash-induced absorption changes of pyranine in AR4 suspension. The sample was measured in 100 mM NaCl and 20 mM KCl.

It is known that at lower pH the time sequence of proton release and uptake is reversed in BR (39,44). An interesting question thus arises: will a higher pH alter the time sequence of proton release and uptake in AR4? The pH-dependence of proton release and uptake in AR4 from pH 7.5 to pH 8.2 was then examined using pyranine as shown in Fig. 1 *B*. This dye has a pK_a of 7.2 at the salt concentration that we have used, which is consistent with the data of Govindjee et al. (59). As shown in Fig. 1 *B*, the temporal order of proton uptake and release was not reversed up to pH 8.2. The different amplitudes of the signal are due to the changes of the sensitivity of pyranine and the different buffering capacity of the sample at different pH levels. The temporal order of proton uptake and release of AR4 was not altered upon increase of salt concentration to 1 M.

To examine the pH-dependence of light-induced proton release and uptake at pH higher than 8.2, we used another pH-sensitive dye, thymol blue with a pK_a of 8.8. We also measured the kinetics of light-induced proton pumping by BR with thymol blue at alkaline pHs. As expected, the measurements show that proton uptake in BR follows proton release at alkaline pHs. So, thymol blue is suitable for measuring the proton pump at high pHs.

As shown in Fig. 2, the temporal order of release and uptake in AR4 was altered in the pH range between 8.0 and 9.0. It should be noted that an increase of absorption of thymol blue at 456 nm means medium acidification, whereas a decrease represents alkalinization, opposite to pyranine. At pHs above 8.6, the increase of absorption of the dye indicates that proton release is followed by proton uptake. The temporal sequence is thus reversed if the medium pH is sufficiently high. The pK_a of proton release complex of AR4 in the M-intermediate was estimated as 8.4 ± 0.2. After 10 mM Tris-HCl buffer (pH 8.8) was added to the system, the signal disappeared, which proves that the signal in Fig. 2 comes from transient proton release and uptake of AR4.

Absorption spectra

Since the carotenoids in the claret membranes are hard to remove and have a large absorbance, it is difficult to isolate the absorption spectrum of the AR4 pigment. The light-adapted absorption spectra of the AR4 claret membrane (Fig. 3 *A*) are very similar to those of the AR1 and AR2 claret membranes (5). Three carotenoids absorption peaks were at 477, 507, and 543 nm. To determine the absorption maximum of AR4, the light-induced absorption changes accompanying transformation of AR4 to the M-intermediate were measured at every 10 nm between 350 and 720 nm. The absorption changes show that the absorption maximum of AR4 is ~565 nm (Fig. 3 *B*), which is very close to that of BR (568 nm), AR1 (568 nm), and AR2 (565 nm) (51). The slight blue shift compared to BR might originate from the Met-145 → Phe replacement (60).

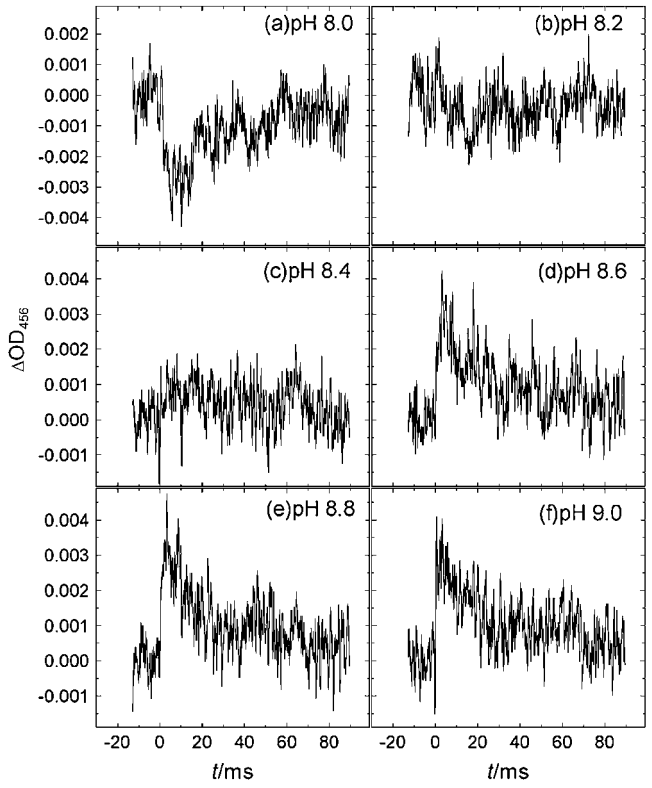

FIGURE 2 pH-dependence of flash-induced absorption changes of thymol blue in suspensions of AR4 at different pHs, detected at 456 nm. The absorption changes were obtained as a difference between traces taken after and before addition of thymol blue. The increase of absorption corresponds to acidification of the medium (proton release), whereas the decrease corresponds to proton uptake. The sample was measured in 100 mM NaCl and 20 mM KCl. The molar concentration of thymol blue is 0.03 mM, 2–3 times of that of AR4.

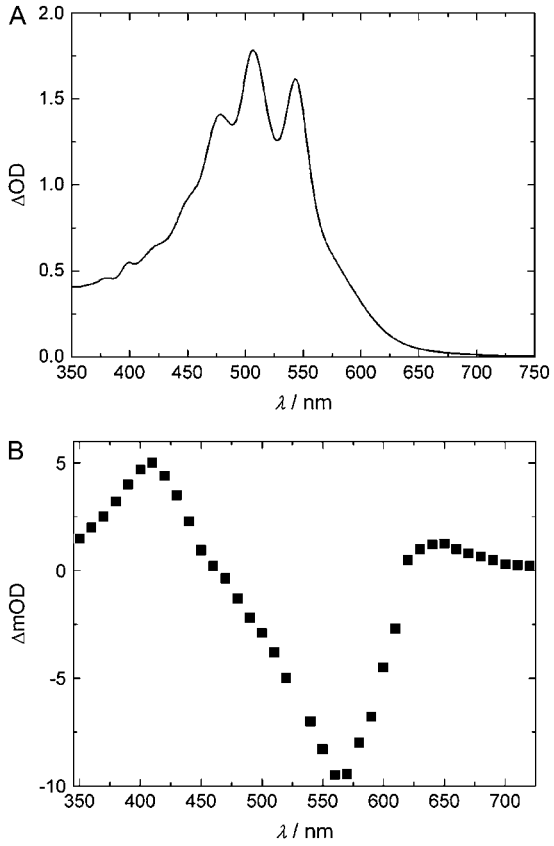

FIGURE 3 (*A*) Absorption spectra of light-adapted AR4. (*B*) Wavelength dependence of the maximum light-induced absorption changes of AR4, measured every 10 nm from 350 to 720 nm (pH 6.8, 75 mM K_2SO_4, 20°C).

Purple-to-blue transition (pK_a of Asp-85)

As in BR, decreasing the pH from 6.9 to 2.05 causes a red shift of the absorption maximum of dark-adapted AR4 due to the purple-to-blue transition associated with protonation of Asp-85 (Fig. 4 *A*) (41,61). A plot of the absorption changes at 660 nm (which are proportional to the fraction of blue membrane and therefore the fraction of protonated Asp-85) versus pH gives a titration curve for Asp-85, which can be best fitted by the Henderson-Hasselbalch equation with a pK_a of 3.6 ($n = 0.9$) (Fig. 4 *B*). This result differs from that for BR, which shows a pK_a of 2.6 ($n = 1.6$) for the purple-to-blue transition (42).

Photocycle reactions in AR4

Light-induced absorption changes of AR4 and BR at 410, 580, and 660 nm are shown in Fig. 5. AR4 shows a faster photocycle than BR, especially M-decay. The trace at 410 nm indicates the decay of the M-intermediate and occurs with two time constants, 0.55 and 3 ms (vs. 3 and 10 ms in BR). The recovery of the initial state (monitored at 580 nm) proceeds with three apparent time constants: 0.6, 3, and 10 ms. The faster component of the 580 recovery and M-decay corresponds to reprotonation of the Schiff base during the M→N transition which occurs 4× faster in AR4 than in BR. The formation and decay of the O-intermediate occurs with apparent time constants of 1.5 and 10 ms, respectively. Below we examine the pH-dependence of the kinetics of the formation and decay of the M- and O-intermediates in AR4 which provides information of the coupling with the protonation states of the groups involved in proton release and uptake.

pH-dependence of M-formation

In WT BR, deprotonation of PRC in the initial state at high pH accelerates M-formation, presumably by elevating the pK_a of proton acceptor (Asp-85 in BR) (45); thus we can measure the pK_a of XH. Such an acceleration is absent in the E204Q (33) and E194C mutants of BR and correlates with the absence of early proton release in these two pigments (34). As shown in Fig. 6 *A*, the kinetics of formation of the M-intermediate are highly pH dependent. M-formation becomes faster at alkaline pH as it does in WT BR (62).

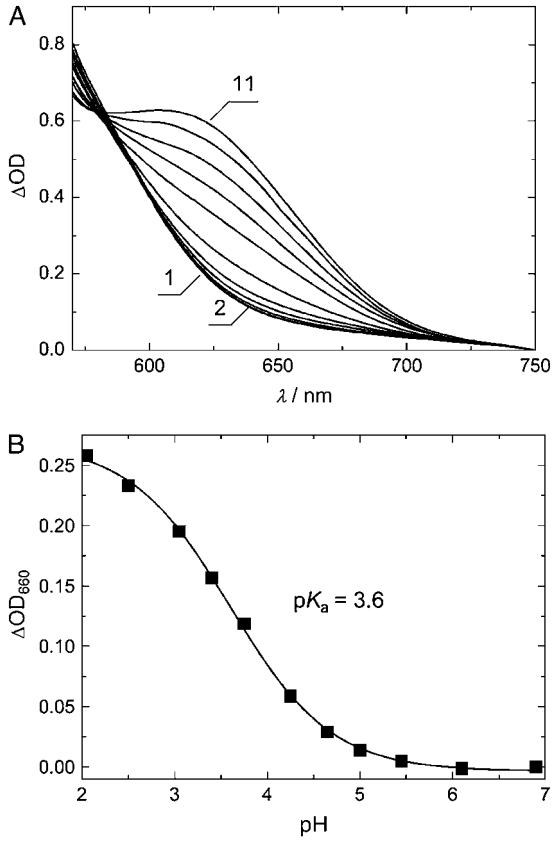

FIGURE 4 (*A*) Absorption spectra of dark-adapted claret membranes (75 mM K_2SO_4, 20°C). Spectra 1–11 were measured at pH 6.90, 6.10, 5.45, 5.00, 4.65, 4.25, 3.75, 3.40, 3.05, 2.50, and 2.05, respectively. (*B*) The pH-dependence of the absorption changes due to the purple-to-blue transition measured at 660 nm. The data were fitted by the Henderson-Hasselbalch equation, $y = A_2 + (A_1 - A_2)/[1 + 10^{n(x-pK)}]$ with a pK_a of 3.6 ($n = 0.9$).

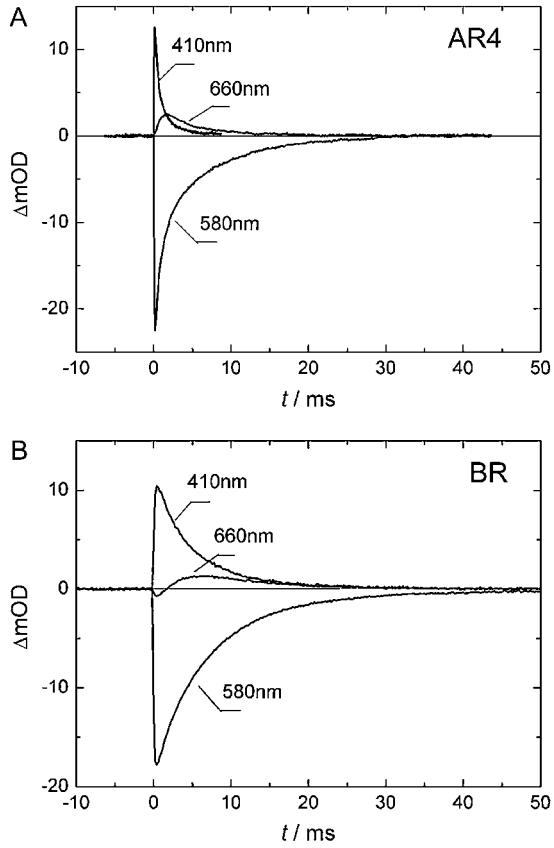

FIGURE 5 Kinetics of the flash-induced absorption changes in (*A*) AR4 and (*B*) BR at the wavelengths indicated (pH 6.9, 75 mM K_2SO_4, 20°C).

This indicates that although early proton release is absent, the PRC is still present in AR4 and its deprotonation in the pigment's initial state affects the proton affinity of the primary proton acceptor from the Schiff base.

Fig. 6 *B* shows the pH-dependence of the fraction of the fast component during M-rise for AR4. The pK_a of the PRC of BR in its initial state, determined from the titration of Asp-85 and the pH-dependence of dark adaptation (42), is ~0.7 pK units higher than the value obtained from pH-dependence of M-rise (9.7 vs. 9.0) (62). Assuming that a similar relationship holds for AR4, the pK_a of XH in the ground state or initial state of AR4 is estimated as 9.7 + 0.7 = 10.4. The pK_a of the PRC in the initial state of BR can be determined either by direct titration of the blue-to-purple transition which is associated with deprotonation of Asp-85 or from pH-dependence of dark adaptation (42). These two methods could not be used for AR4, because of a very small amount of blue membrane at pHs above 6 and the small absorption changes due to dark adaptation. The presence of carotenoids in the claret membrane and their perturbation upon titration was also a complication. However a third method involving the pH-dependence of M-rise produced a clear result indicating that the PRC has a pK_a ~10.4 in the initial state.

pH-dependence of O-formation and decay

The pH-dependence of the fraction of O-intermediate and of the rate constants of its formation and decay contain information on the pK_a of the groups involved in proton release and uptake (57). As seen in Fig. 7 *A*, the pH-dependence of the fraction of O-intermediate in AR4 is similar to that in BR, but each of the two pK_as are shifted to higher values. The fraction of O decreases with two pK_as of 5.8 and 9.2 vs. 3.9 and 7.5 in BR, respectively (57). The pK_a of 5.8 is related to the pK_a of the XH in O, and the pK_a of 9.2 is apparently close to the pK_a of Asp-96 in AR4, as suggested by Balashov et al. for analogous pK_a of 7.5 in BR (57). The pH dependencies of the apparent rate constants of O-rise and O-decay for AR4 are shown in Fig. 7 *B*. Both rate constants decrease as the pH decreases below 7 with a pK_a of ~6.5, which would be the pK_a of the proton release group in the O-intermediate (57). The apparent constant of O-decay decreases at high pH with pK_a of 8.4–8.8 which we attribute to the pK_a of the proton donor during proton uptake (19,57). It should be noted that the rate constants are rather sensitive to measurement

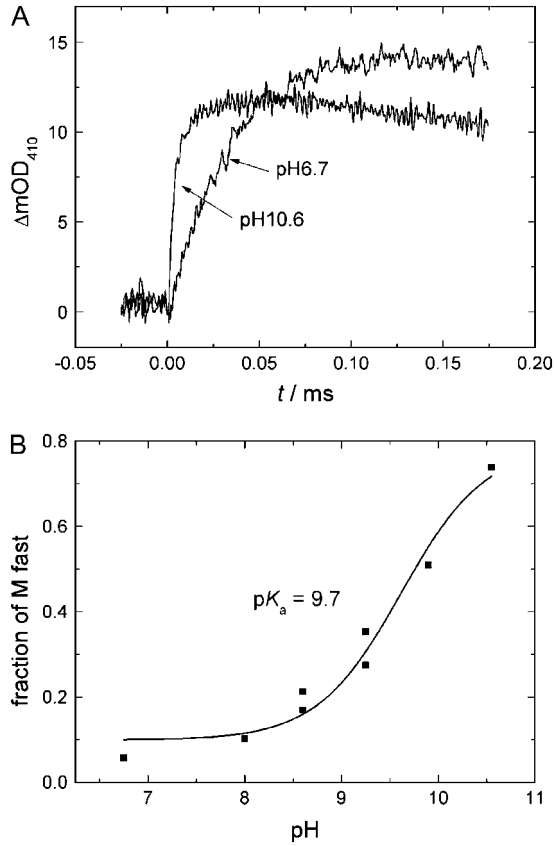

FIGURE 6 (*A*) M-formation of AR4 at the pHs indicated. (*B*) pH-dependence of the fraction of the fast component of M-formation of AR4. The samples were measured in gels at the given pHs. The fitted curve gives $pK_a \sim 9.7$.

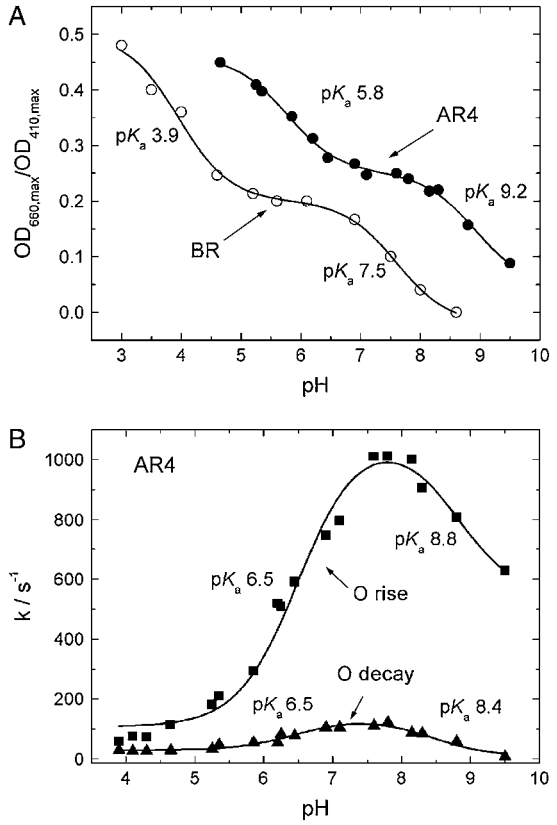

FIGURE 7 (*A*) pH-dependence of the normalized O-intermediate (maximum light-induced absorption change at 660 nm due to the formation of the O-intermediate divided by maximum absorption change at 410 nm due to the M-intermediate at the associated pH) in both AR4 and BR. (*B*) The pH-dependence of the apparent rate constants of O-formation and O-decay in AR4 (75 mM K_2SO_4, 20°C). The rate constants of O-rise and decay together with the O-amplitude were fitted with the equation $y = A_0[k_1/(k_1 - k_2)](e^{-k_2 x} - e^{-k_1 x})$, assuming an unidirectional N→O→BR transition and ignoring the possibility of a N↔O back reaction (57).

conditions such as pH and medium composition, so it is only meaningful to compare data from identical samples.

Correlation of proton uptake and release with kinetics of the O-intermediate in AR4

To elucidate the relationship between the kinetics of proton transfer and the intermediates in the photocycle of AR4, we compared O_{640} kinetics with those of proton uptake and release as shown in Fig. 8. Fig. 8 indicates that proton uptake and proton release correspond to O-formation and O-decay, respectively. This situation is consistent with the proton pumping kinetics of BR at pH < 5.7, where proton release is followed by uptake and correlates with the last transition of the photocycle, O → BR (39).

The relaxation time for proton release in AR4 around neutral pH is consistent with that for O-decay (see also Fig. 8). In WT BR (57,63,64), O-rise and decay are decided by two proton transfer steps: proton uptake by Asp-96, and proton transfer from Asp-85 to the PRC. But in AR4 at pH 7, fast proton release does not occur and late proton release happens during O-decay, apparently being coupled to the deprotonation of the primary proton acceptor (Asp-85).

DISCUSSION

About the temporal order of proton uptake and release

After the first proton transfer from the Schiff base to Asp-85, the remaining proton transfer events during the photocycle of a retinal-based proton pump can be divided into two parts: one is along the half channel on the extracellular side, which leads to release of a proton; the other is along other half channel on the cytoplasmic side, which leads to uptake of another proton. In the photocycle of AR4, light-induced proton release lags behind proton uptake, which is opposite to the ''normal'' temporal order in BR (proton release preceding proton uptake) at neutral pH. In principle, the reversed order might result from either acceleration of proton uptake or delay of proton release (or both). It is known that proton uptake occurs during the N-to-O transition or between two N-substates (40) and thus should be during or after M-decay. So, proton uptake cannot be very fast. So the

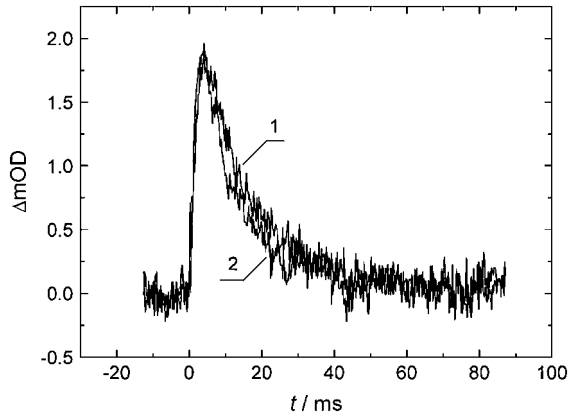

FIGURE 8 Kinetics of the flash-induced absorption changes of the pH-sensitive dye pyranine at 458 nm (1) and of the O-intermediate at 660 nm (2) in a suspension of AR4 (pH 7.1, 75 mM K_2SO_4, 20°C). The two-component fit of the traces gives similar apparent time constants for the O-rise and proton uptake (1.7 ± 0.2 ms) and close time constants for O-decay (11 ms) and proton release (14 ms).

origin of the reversed temporal order is the delay of proton release.

Mechanism of proton release in AR4

Now, the question becomes why proton release in AR4 is delayed. The näive interpretation might be disruption of the PRC in AR4, similar to what occurs in the E204Q (33) and E194C (34) mutants of BR. However, if the PRC in AR4 is not a functional unit as in the above BR mutants, then, like E204Q and E194C, we should not observe any pH-dependence of kinetics of M-formation. Moreover, the time constant for the turnover of the photocycle would be in the range of 100 ms, as in the E204Q mutant (57). In contrast to this, we observed a striking pH-dependence of M-rise (Fig. 6) and a relatively fast photocycle (Fig. 5). The possibility of a lack of an intact PRC is thus ruled out.

In the case of BR, the order of proton release and uptake can be reversed by decreasing the medium pH sufficiently (44). When the medium pH is lower than the pK_a of PRC in WT BR (<5.7), the PRC is unable to deprotonate. Thus proton release occurs late in the photocycle, during the $O_{640} \rightarrow BR_{570}$ transition (39) when the pK_a of XH decreases to 4.5 (42). Likewise, the temporal order of proton release and uptake in AR4 should be altered if the pH is raised sufficiently above the hypothetical pK_a of the PRC in M of AR4. This phenomenon was found in our experiments where the kinetics of proton pumping were followed up to pH 8.6 (Fig. 2). The pK_a of the PRC in the M-intermediate of AR4 is estimated to be ~8.4. This result strongly supports the idea that the basic proton pumping principle of AR4 is similar to that of BR because the temporal order of proton release and uptake of AR4 can be reversed by just increasing medium pH.

The pH titration experiments allow us to determine the pK_as of several key residues of the proton pump. Table 1 summarizes the pK_a changes.

In the unphotolyzed state of AR4, the pK_a is ~3.6 for Asp-85 and ~10.4 for XH. So the pK_a of Asp-85 in AR4 is one unit higher than that in BR ($pK_a = 2.6$); the pK_a of XH in the ground state of AR4 is also ~0.7 unit higher than in BR ($pK_a = 9.7$). All of the pK_as for Asp-85, XH, and Asp-96 are elevated in AR4, which suggests that AR4 is a proton pump whose operating range is significantly shifted to more alkaline pHs.

The pH-dependence of the fraction of the fast component during M-formation (Fig. 6) indicates that the coupling between Asp-85 and XH still exists in AR4 as in BR (19). But, it has been significantly weakened in AR4. The decrease of the pK_a of XH after AR4 is illuminated is much less (from pK_a 10.4 to 8.4) than that for BR (from pK_a 9.7 to 5.7). The higher pK_a of the PRC in the photocycle does not allow fast proton release at neutral pH. Such a weakened coupling model is schematically indicated in Fig. 9.

In the case of BR, this coupling can also be weakened or blocked in some site-directed mutants. For example, mutagenesis of several different amino acid residues in or around the retinal binding pocket of BR such as Arg-82Ala (46), Arg-82Gln (65), Arg-134His (66) and Lys-129His (59) created a reversed temporal pattern of proton release and uptake (now proton release lagging proton uptake). Hence we propose that weakened coupling is responsible for the lack of early proton release in AR4 and thus the reversed temporal order of proton uptake and proton release. This weakened coupling in AR4 correlates with the elevated pK_a of the proton donor analogous to Asp-96, which might not be an accidental relationship.

Possible residues involved in coupling between Asp-85 and XH in AR4

The coupling in BR can be physically understood from the high-resolution crystal structures of the initial state of BR and the M-intermediate (67,68). In BR, Glu-204, Glu-194, Arg-82 and Asp-85 form a complex hydrogen-bonded

TABLE 1 pK_as Measured from a series of pH titration experiments

	pK_a in AR4	pK_a in BR	
XH in ground state	~10.4	9.7*	Combination of Fig. 6 *B* and corresponding text
XH in M-intermediate	~8.4	5.7†	Fig. 2
XH in O-intermediate	~6.5	4.3‡	Fig. 7 *B*
Asp-85 in ground state	3.6	2.6*	Fig. 4 *B*
Asp-96 during N → O	~9.2	7.5‡	Fig. 7 *A*

*From (42).
†From (39,44).
‡From (57).

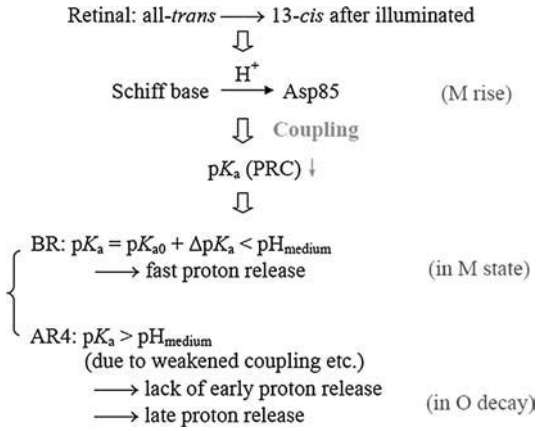

FIGURE 9 Schematic presentation of the coupling between the protonation of Asp-85 and pK_a change of the PRC in M-state. Unlike BR, the pK_a of the PRC in AR4 does not drop low enough to allow early proton release at the neutral pH of the medium due to the weakened coupling.

network incorporating several bound water molecules. The movement of the positive charge of Arg-82 from its inward position to its outward position upon M-formation, accompanied by changes in hydrogen binding of several water molecules, is what apparently underlies the coupling between the protonated state of Asp-85 and proton release site (69–71). In AR4, this coupling relation between Asp-85 and XH is weakened. Several residues close to Glu-194 and Glu-204, part of the PRC, are changed to residues with smaller side groups in AR4. Ile-191, Ile-198 and Ile-203 are all changed to Vals, whereas Pro-200 and Asn-202 are changed to Glys. Tyr-133 and Leu-207 are replaced with Alas. These changes leave more space around the Glu-194/Glu-204 dyad, which therefore might accommodate more water molecules and alter the H-bonded network in this region. The possible new H-bonds might stabilize the Glu-194/Glu-204 dyad in the M-state and increase the energy barrier for the early light-induced proton release, which is probably from the Glu-194/Glu-204 dyad or a nearby water molecule (38,72). Moreover in BR, Pro-77 and Ser-193 are the residues that surround a protonated water cluster, which is important for proton release (38). The replacement of Pro-77 by Asp and Ser-193 by Thr in AR4 might affect the network in the proton release channel.

The reversed temporal order of proton pumping kinetics in AR4 is not the only archaerhodopsin example. A similar

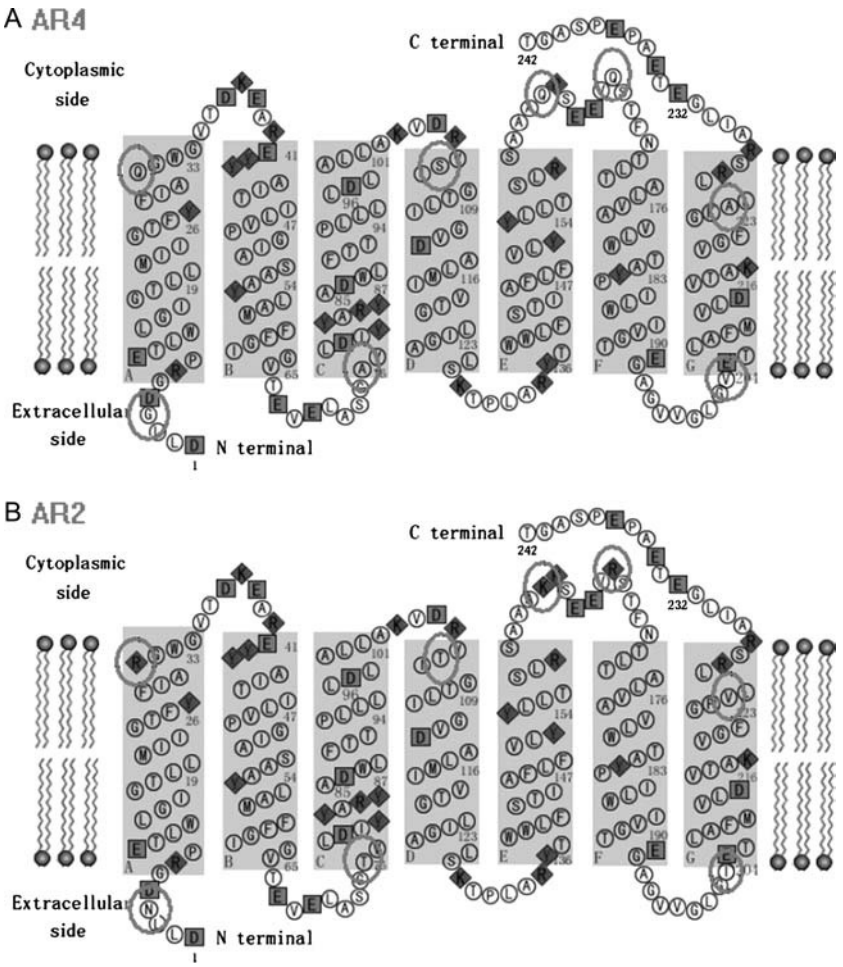

FIGURE 10 Amino acid sequences of (*A*) AR4 (2,3) and (*B*) AR2 (9,75). Squares and diamonds denote acidic residue and alkaline residues, respectively. The eight pairs of residues different between AR2 and AR4 are marked with large circles.

phenomenon was found in AR1 (51). An x-ray crystallographic study of AR shows that the main-chain structures of AR1 and AR2 are similar to that of BR (73,74). The reversion of the order of proton release and uptake in AR1 was attributed to the natural mutation from Lys-129 in BR to His-129 in AR1, for mutation of Lys-129 to His-129 in BR also reversed the normal order (59). This argument however does not work for AR4, which has a lysine at position 129 rather than a histidine.

In contrast to AR4, AR2 exhibits the normal temporal order of light-driven proton pumping kinetics (51). Just eight amino acid residues in AR2 are different from those in AR4 (see Fig. 10), but this seems sufficient to change the proton release/uptake order. Since XH must be located in the half-channel on the extracellular side, the associated three different residues among the eight residues marked in Fig. 10 might be responsible for the change. The most probable candidate is Thr-74, which in AR2 is replaced by an alanine. Threonine is likely to be a part of the hydrogen bond network.

The function of the PRC in AR4

Several observations indicate that the proton release complex, XH is functional in AR4 and catalyzes O-decay (and so recovery of the pigment's initial state), even at neutral pH. First, as in WT BR, the O-intermediate does not accumulate in large amounts (Figs. 5 and 7). This is much different from the behavior of the O-intermediate in the E204Q mutant where the fraction of O is severalfold larger (57). Second, the rate constant of O-formation exhibits a strong pH-dependence with pK_a ~6.5 (Fig. 7). This is similar to WT BR, where an analogous pH-dependence was observed and the O-to-BR transition at low pH was controlled by the protonation state of XH (57). From this we can conclude that the pK_a of XH in O is ~6.5 in AR4, 2 pK units higher than in WT BR. Last but not least, the overall photocycle turnover (Fig. 5 *A*) is close to that of WT BR (Fig. 5 *B*) rather than the E204Q mutant (100 ms), indicating again that the deprotonation of a group analogous to Asp-85 is catalyzed in AR4. Thus the critical role of the PRC in the photocycle is not just in catalyzing early proton release but mainly in catalyzing the deprotonation of primary proton acceptor, facilitating proton transfer in the outward proton channel and recovery of the initial state (shortening turnover of the photocycle).

In summary, this work examines the photochemical reactions of AR4 with emphasis of their pH dependencies. By studying the features of AR4 and performing comparisons, we conclude that AR4 is a light-driven proton pump like BR, but with the pK_as of the key groups shifted to a more alkaline pH range. The temporal order of proton uptake and release in AR4 can be reversed to that in BR when the pH is increased to 8.6. Although proton release is delayed till the end of the photocycle at neutral pH, it still occurs through the PRC, which is different from the behavior of several mutants of BR in which PRC is disabled. Our analysis indicates that the PRC in AR4 facilitates deprotonation of Asp-85 in the final step of the photocycle. Weakened coupling between Asp-85 and XH is assumed to account for the lack of early proton release and thus the reversed temporal order. Some key residues potentially responsible for this coupling have been suggested.

This work was supported by National Science Foundation of China (Nos. 20374015, 20574013, 50533010, and a Two-Base Grant), the Key Grant of Chinese Ministry of Education (No. 305004), the Award Foundation for Young Teachers from Chinese Ministry of Education, 973 project (No. 2005CB522700), and 863 Project from Chinese Ministry of Science and Technology, Science and Technology Developing Foundation of Shanghai (Nos. 04JC14019 and 055207082); and National Institutes of Health grant GM 52023 (to T.G.E. and S.P.B.).

REFERENCES

1. Li, Q. G., Q. G. Sun, W. Zhao, H. Wang, and D. Q. Xu. 2000. Newly isolated archaerhodopsin from a strain of Chinese halobacteria and its proton pumping behavior. *Biochim. Biophys. Acta.* 1466:260–266.
2. Wang, H., S. X. Zhan, Q. G. Sun, D. Q. Xu, W. Zhao, W. D. Huang, and Q. G. Li. 2000. Primary structure of helix C to helix G of a new retinal protein in *H.sp.xz515*. *Chin. Sci. Bull.* 45:1108–1113.
3. Wang, Y. R., J. Hong, M. Ming, J. D. Ding, Q. G. Li, and W. D. Huang. 2003. Rapid cloning of an archaerhodopsin gene from Halobacterium species xz515 by LPA. *J. Fudan University.* 42: 577–583.
4. Mukohata, Y. 1994. Comparative-studies on ion pumps of the bacterial rhodopsin family. *Biophys. Chem.* 50:191–201.
5. Mukohata, Y., Y. Sugiyama, K. Ihara, and M. Yoshida. 1988. An Australian halobacterium contains a novel proton pump retinal protein: archaerhodopsin. *Biochem. Biophys. Res. Commun.* 151:1339–1345.
6. Mukohata, Y., K. Ihara, K. Uegaki, Y. Miyashita, and Y. Sugiyama. 1991. Australian halobacteria and their retinal-protein ion pumps. *Photochem. Photobiol.* 54:1039–1045.
7. Sugiyama, Y., M. Maeda, M. Futai, and Y. Mukohata. 1989. Isolation of a gene that encodes a new retinal protein, archaerhodopsin, from *Halobacterium sp. aus-1*. *J. Biol. Chem.* 264:20859–20862.
8. Ihara, K., T. Umemura, I. Katagiri, T. Kitajima-Ihara, Y. Sugiyama, Y. Kimura, and Y. Mukohata. 1999. Evolution of the archaeal rhodopsins: evolution rate changes by gene duplication and functional differentiation. *J. Mol. Biol.* 285:163–174.
9. Brown, L. S. 2001. Proton transport mechanism of bacteriorhodopsin as revealed by site-specific mutagenesis and protein sequence variability. *Biochemistry. (Moscow).* 66:1249–1255.
10. Lanyi, J. K. 2004. Bacteriorhodopsin. *Annu. Rev. Physiol.* 66:665–688.
11. Haupts, U., J. Tittor, and D. Oesterhelt. 1999. Closing in on bacteriorhodopsin: Progress in understanding the molecule. *Annu. Rev. Biophys. Biomol. Struct.* 28:367–399.
12. Ebrey, T. G. 1993. Light energy transduction in bacteriorhodopsin. *In* Thermodynamics of Membrane Receptors and Channels. M. B. Jackson, editor. CRC Press, Boca Raton, FL. 353–387.
13. Hampp, N. 2000. Bacteriorhodopsin as a photochromic retinal protein for optical memories. *Chem. Rev.* 100:1755–1776.
14. Birge, R. R. 1990. Nature of the primary photochemical events in rhodopsin and bacteriorhodopsin. *Biochim. Biophys. Acta.* 1016: 293–327.
15. Lanyi, J. K. 2001. X-ray crystallography of bacteriorhodopsin and its photointermediates: insights into the mechanism of proton transport. *Biochemistry (Moscow).* 66:1192–1196, and other articles in this issue.
16. Lanyi, J. K. 2000. Bacteriorhodopsin. *Biochim. Biophys. Acta.* 1460: 1–3, and other articles in this issue.

17. Lozier, R. H., R. A. Bogomolni, and W. Stoeckenius. 1975. Bacteriorhodopsin: a light-driven proton pump in *Halobacterium halobium*. *Biophys. J.* 15:955–963.

18. Lanyi, J. K. 1993. Proton translocation mechanism and energetics in the light-driven pump bacteriorhodopsin. *Biochim. Biophys. Acta.* 1183: 241–261.

19. Balashov, S. P. 2000. Protonation reactions and their coupling in bacteriorhodopsin. *Biochim. Biophys. Acta.* 1460:75–94.

20. Herzfeld, J., and J. C. Lansing. 2002. Magnetic resonance studies of the bacteriorhodopsin pump cycle. *Annu. Rev. Biophys. Biomol. Struct.* 31:73–95.

21. Lanyi, J. K., and B. Schobert. 2003. Mechanism of proton transport in bacteriorhodopsin from crystallographic structures of the K, L, M-1, M-2, and M-2' intermediates of the photocycle. *J. Mol. Biol.* 328: 439–450.

22. Kahya, N., D. A. Wiersma, B. Poolman, and D. Hoekstra. 2002. Spatial organization of bacteriorhodopsin in model membranes: Light-induced mobility changes. *J. Biol. Chem.* 277:39304–39311.

23. Abdulaev, N. G., T. T. Strassmaier, T. Ngo, R. W. Chen, H. Luecke, D. D. Oprian, and K. D. Ridge. 2002. Grafting segments from the extracellular surface of CCR5 onto a bacteriorhodopsin transmembrane scaffold confers HIV-1 coreceptor activity. *Structure.* 10:515–525.

24. Xie, A. H., A. F. G. van der Meer, and R. H. Austin. 2002. Excited-state lifetimes of far-infrared collective modes in proteins. *Phys. Rev. Lett.* 88:018101–018104.

25. Shih, A. Y., I. G. Denisov, J. C. Phillips, S. G. Sligar, and K. Schulten. 2005. Molecular dynamics simulations of discoidal bilayers assembled from truncated human lipoproteins. *Biophys. J.* 88:548–556.

26. Deverall, M. A., E. Gindl, E. K. Sinner, H. Besir, J. Ruehe, M. J. Saxton, and C. A. Naumann. 2005. Membrane lateral mobility obstructed by polymer-tethered lipids studied at the single molecule level. *Biophys. J.* 88:1875–1886.

27. Janovjak, H., D. J. Muller, and A. D. L. Humphris. 2005. Molecular force modulation spectroscopy revealing the dynamic response of single bacteriorhodopsins. *Biophys. J.* 88:1423–1431.

28. Oka, T., K. Inoue, M. Kataoka, and N. Yagi. 2005. Structural transition of bacteriorhodopsin is preceded by deprotonation of Schiff base: microsecond time-resolved x-ray diffraction study of purple membrane. *Biophys. J.* 88:436–442.

29. Mason, A. J., S. L. Grage, S. K. Straus, C. Glaubitz, and A. Watts. 2004. Identifying anisotropic constraints in multiply labeled bacteriorhodopsin by N-15 MAOSS NMR: a general approach to structural studies of membrane proteins. *Biophys. J.* 86:1610–1617.

30. Liu, S. Y. 1990. Light-induced currents from oriented purple membrane. 1. Correlation of the microsecond component (B2) with the L-M photocycle transition. *Biophys. J.* 57:943–950.

31. Heberle, J., and N. A. Dencher. 1992. Surface-bound optical probes monitor proton translocation and surface-potential changes during the bacteriorhodopsin photocycle. *Proc. Natl. Acad. Sci. USA.* 89:5996–6000.

32. Cao, Y., L. S. Brown, J. Sasaki, A. Maeda, R. Needleman, and J. K. Lanyi. 1995. Relationship of proton release at the extracellular surface to deprotonation of the Schiff-base in the bacteriorhodopsin photocycle. *Biophys. J.* 68:1518–1530.

33. Brown, L. S., J. Sasaki, H. Kandori, A. Maeda, R. Needleman, and J. K. Lanyi. 1995. Glutamic-acid-204 is the terminal proton release group at the extracellular surface of bacteriorhodopsin. *J. Biol. Chem.* 270: 27122–27126.

34. Balashov, S. P., E. S. Imasheva, T. G. Ebrey, N. Chen, D. R. Menick, and R. K. Crouch. 1997. Glutamate-194 to cysteine mutation inhibits fast light-induced proton release in bacteriorhodopsin. *Biochemistry.* 36:8671–8676.

35. Dioumaev, A. K., H. T. Richter, L. S. Brown, M. Tanio, S. Tuzi, H. Saito, Y. Kimura, R. Needleman, and J. K. Lanyi. 1998. Existence of a proton transfer chain in bacteriorhodopsin: participation of Glu-194 in the release of protons to the extracellular surface. *Biochemistry.* 37: 2496–2506.

36. Luecke, H., H. T. Richter, and J. K. Lanyi. 1998. Proton transfer pathways in bacteriorhodopsin at 2.3 Angstrom resolution. *Science.* 280:1934–1937.

37. Rammelsberg, R., G. Huhn, M. Lubben, and K. Gerwert. 1998. Bacteriorhodopsin's intramolecular proton-release pathway consists of a hydrogen-bonded network. *Biochemistry.* 37:5001–5009.

38. Garczarek, F., L. S. Brown, J. K. Lanyi, and K. Gerwert. 2005. Proton binding within a membrane protein by a protonated water cluster. *Proc. Natl. Acad. Sci. USA.* 102:3633–3638.

39. Cao, Y., L. S. Brown, R. Needleman, and J. K. Lanyi. 1993. Relationship of proton uptake on the cytoplasmic surface and reisomerization of the retinal in the bacteriorhodopsin photocycle—an attempt to understand the complex kinetics of the pH changes and the N- and O-intermediates. *Biochemistry.* 32:10239–10248.

40. Dioumaev, A. K., L. S. Brown, R. Needleman, and J. K. Lanyi. 2001. Coupling of the reisomerization of the retinal, proton uptake, and reprotonation of Asp-96 in the N-photointermediate of bacteriorhodopsin. *Biochemistry.* 40:11308–11317.

41. Metz, G., F. Siebert, and M. Engelhard. 1992. Asp-85 is the only internal aspartic-acid that gets protonated in the M-intermediate and the purple-to-blue transition of bacteriorhodopsin —a solid-state C-13 Cp-Mas NMR investigation. *FEBS Lett.* 303:237–241.

42. Balashov, S. P., E. S. Imasheva, R. Govindjee, and T. G. Ebrey. 1996. Titration of aspartate-85 in bacteriorhodopsin: what it says about chromophore isomerization and proton release. *Biophys. J.* 70:473–481.

43. Braiman, M. S., A. K. Dioumaev, and J. R. Lewis. 1996. A large photolysis-induced pK_a increase of the chromophore counterion in bacteriorhodopsin: implications for ion transport mechanisms of retinal proteins. *Biophys. J.* 70:939–947.

44. Zimanyi, L., G. Varo, M. Chang, B. F. Ni, R. Needleman, and J. K. Lanyi. 1992. Pathways of proton release in the bacteriorhodopsin photocycle. *Biochemistry.* 31:8535–8543.

45. Balashov, S. P., R. Govindjee, E. S. Imasheva, S. Misra, T. G. Ebrey, Y. Feng, R. K. Crouch, and D. R. Menick. 1995. The two pK_a of aspartate-85 and control of thermal-isomerization and proton release in the Arginine-82 to Lysine mutant of bacteriorhodopsin. *Biochemistry.* 34:8820–8834.

46. Balashov, S. P., R. Govindjee, M. Kono, E. Imasheva, E. Lukashev, T. G. Ebrey, R. K. Crouch, D. R. Menick, and Y. Feng. 1993. Effect of the Arginine-82 to Alanine mutation in bacteriorhodopsin on dark-adaptation, proton release, and the photochemical cycle. *Biochemistry.* 32:10331–10343.

47. Richter, H. T., L. S. Brown, R. Needleman, and J. K. Lanyi. 1996. A linkage of the pK_as of Asp-85 and Glu-204 forms part of the reprotonation switch of bacteriorhodopsin. *Biochemistry.* 35:4054–4062.

48. Lanyi, J. K., and B. Schobert. 2004. Local-global conformational coupling in a heptahelical membrane protein: transport mechanism from crystal structures of the nine states in the bacteriorhodopsin photocycle. *Biochemistry.* 43:3–8.

49. Becher, B. M., and J. Y. Cassim. 1975. Improved isolation procedures for the purple membrane of *Halobacterium halobium*. *Prep. Biochem.* 5:161–178.

50. Oesterhelt, D., and W. Stoeckenius. 1974. Isolation of the cell membrane of Halobacterium halobium and its fraction into red and purple membrane. *Methods Enzymol.* 31:667–678.

51. Lukashev, E. P., R. Govindjee, M. Kono, T. G. Ebrey, Y. Sugiyama, and Y. Mukohata. 1994. pH-dependence of the absorption-spectra and photochemical-transformations of the archaerhodopsins. *Photochem. Photobiol.* 60:69–75.

52. Wang, N., and Q. G. Li. 1986. The microcomputer-controlled kinetic spectrophotometer in millisecond timescale and its application to the observation of the bacteriorhodopsin photocycle. *Acta. Biochim. Biophys. Sin.* 2:32–36.

53. Huang, L., M. Ming, J. Liu, Q. G. Li, and J. D. Ding. 2003. Preparation of liposome containing bacteriorhodopsin with ''natural'' preferred

orientation and detection of its transient photoresponse. *Acta Biochim. Biophys. Sin.* 35:391–395.

54. Liu, J., M. Ming, L. Huang, Q. G. Li, and J. D. Ding. 2002. Preparation and study of bacteriorhodopsin/poly(vinyl alcohol) composite film. *Acta. Chim. Sin.* 60:2209–2213.
55. Wu, J., L. Huang, J. Liu, M. Ming, Q. G. Li, and J. D. Ding. 2005. Directional self-assembly in archaerhodopsin-reconstituted phospholipid liposomes. *Chin. J. Chem.* 23:330–333.
56. Govindjee, R., T. G. Ebrey, and A. R. Crofts. 1980. The quantum efficiency of proton pumping by the purple membrane of *Halobacterium halobium*. *Biophys. J.* 30:231–242.
57. Balashov, S. P., M. Lu, E. S. Imasheva, R. Govindjee, T. G. Ebrey, B. Othersen, Y. M. Chen, R. K. Crouch, and D. R. Menick. 1999. The proton release group of bacteriorhodopsin controls the rate of the final step of its photocycle at low pH. *Biochemistry.* 38:2026–2039.
58. Liu, S. Y., M. Kono, and T. G. Ebrey. 1991. Effect of pH buffer molecules on the light-induced currents from oriented purple membrane. *Biophys. J.* 60:204–216.
59. Govindjee, R., E. S. Imasheva, S. Misra, S. P. Balashov, T. G. Ebrey, N. Chen, D. R. Menick, and R. K. Crouch. 1997. Mutation of a surface residue, Lysine-129, reverses the order of proton release and uptake in bacteriorhodopsin; Guanidine hydrochloride restores it. *Biophys. J.* 72:886–898.
60. Ihara, K., T. Amemiya, Y. Miyashita, and Y. Mukohata. 1994. Met-145 is a key residue in the dark-adaptation of bacteriorhodopsin homologs. *Biophys. J.* 67:1187–1191.
61. Subramaniam, S., T. Marti, and H. G. Khorana. 1990. Protonation state of Asp (Glu)-85 regulates the purple-to-blue transition in bacteriorhodopsin mutants Arg-82-Ala and Asp-85-Glu—the blue form is inactive in proton translocation. *Proc. Natl. Acad. Sci. USA.* 87:1013–1017.
62. Balashov, S. P., R. Govindjee, and T. G. Ebrey. 1991. Red shift of the purple membrane absorption-band and the deprotonation of tyrosine residues at high pH—origin of the parallel photocycles of trans-bacteriorhodopsin. *Biophys. J.* 60:475–490.
63. Li, Q., S. Bressler, D. Ovrutsky, M. Ottolenghi, N. Friedman, and M. Sheves. 2000. On the protein residues that control the yield and kinetics of O-630 in the photocycle of bacteriorhodopsin. *Biophys. J.* 78: 354–362.
64. Misra, S., R. Govindjee, T. G. Ebrey, N. Chen, J. X. Ma, and R. K. Crouch. 1997. Proton uptake and release are rate-limiting steps in the photocycle of the bacteriorhodopsin mutant E204Q. *Biochemistry.* 36:4875–4883.
65. Govindjee, R., S. Misra, S. P. Balashov, T. G. Ebrey, R. K. Crouch, and D. R. Menick. 1996. Arginine-82 regulates the pK_a of the group responsible for the light-driven proton release in bacteriorhodopsin. *Biophys. J.* 71:1011–1023.
66. Lu, M., S. P. Balashov, T. G. Ebrey, N. Chen, Y. M. Chen, D. R. Menick, and R. K. Crouch. 2000. Evidence for the rate of the final step in the bacteriorhodopsin photocycle being controlled by the proton release group: R134H mutant. *Biochemistry.* 39:2325–2331.
67. Luecke, H., B. Schobert, H. T. Richter, J. P. Cartailler, and J. K. Lanyi. 1999. Structural changes in bacteriorhodopsin during ion transport at 2 Angstrom resolution. *Science.* 286:255–260.
68. Luecke, H., B. Schobert, H. T. Richter, J. P. Cartailler, and J. K. Lanyi. 1999. Structure of bacteriorhodopsin at 1.55 angstrom resolution. *J. Mol. Biol.* 291:899–911.
69. Luecke, H., B. Schobert, J. P. Cartailler, H. T. Richter, A. Rosengarth, R. Needleman, and J. K. Lanyi. 2000. Coupling photoisomerization of retinal to directional transport in bacteriorhodopsin. *J. Mol. Biol.* 300:1237–1255.
70. Tanimoto, T., M. Shibata, M. Belenky, J. Herzfeld, and H. Kandori. 2004. Altered hydrogen bonding of Arg-82 during the proton pump cycle of bacteriorhodopsin: a low-temperature polarized FTIR spectroscopic study. *Biochemistry.* 43:9439–9447.
71. Xiao, Y. W., M. S. Hutson, M. Belenky, J. Herzfeld, and M. S. Braiman. 2004. Role of Arginine-82 in fast proton release during the bacteriorhodopsin photocycle: a time-resolved FT-IR study of purple membranes containing N-15-labeled Arginine. *Biochemistry.* 43:12809–12818.
72. Grudinin, S., G. Buldt, V. Gordeliy, and A. Baumgaertner. 2005. Water molecules and hydrogen-bonded networks in bacteriorhodopsin—molecular dynamics simulations of the ground state and the M-intermediate. *Biophys. J.* 88:3252–3261.
73. Enami, N., H. Okumura, and T. Kouyama. 2002. X-ray crystallographic study of archaerhodopsin. *J. Photosci.* 9:320–322.
74. Yoshimura, K., N. Enami, H. Okumura, M. Murakami, K. Ihara, and T. Kouyama. 2004. Crystal structure of archaerhodopsin-2 at 2.6A resolution. http://bsr2004.spring8.or.jp/pdfs/abst74.pdf.
75. Uegaki, K., Y. Sugiyama, and Y. Mukohata. 1991. Archaerhodopsin-2, from *Halobacterium sp Aus-2* further reveals essential amino-acid-residues for light-driven proton pumps. *Arch. Biochem. Biophys.* 286: 107–110.